BRAIN
ORIGINAL ARTICLE

De novo FZR1 loss-of-function variants cause developmental and epileptic encephalopathies

Sathiya N. Manivannan,[1,2] Jolien Roovers,[3,4] Noor Smal,[5] Candace T. Myers,[6] Dilsad Turkdogan,[7] Filip Roelens,[8] Oguz Kanca,[1,2] Hyung-Lok Chung,[1,2] Tasja Scholz,[9] Katharina Hermann,[10] Tatjana Bierhals,[9] Hande S. Caglayan,[11] Hannah Stamberger,[5,12] MAE Working Group of EuroEPINOMICS RES Consortium, Heather Mefford,[6] Peter de Jonghe,[3,4,12] Shinya Yamamoto,[1,2,13,14,15] Sarah Weckhuysen[5,12,16,17] and Hugo J. Bellen[1,2,13,14,15,18]

FZR1, which encodes the Cdh1 subunit of the anaphase-promoting complex, plays an important role in neurodevelopment by regulating the cell cycle and by its multiple post-mitotic functions in neurons. In this study, evaluation of 250 unrelated patients with developmental and epileptic encephalopathies and a connection on GeneMatcher led to the identification of three *de novo* missense variants in *FZR1*.

Whole-exome sequencing in 39 patient–parent trios and subsequent targeted sequencing in an additional cohort of 211 patients was performed to identify novel genes involved in developmental and epileptic encephalopathy. Functional studies in *Drosophila* were performed using three different mutant alleles of the *Drosophila* homologue of *FZR1 fzr*.

All three individuals carrying *de novo* variants in *FZR1* had childhood-onset generalized epilepsy, intellectual disability, mild ataxia and normal head circumference. Two individuals were diagnosed with the developmental and epileptic encephalopathy subtype myoclonic atonic epilepsy. We provide genetic-association testing using two independent statistical tests to support *FZR1* association with developmental and epileptic encephalopathies. Further, we provide functional evidence that the missense variants are loss-of-function alleles using *Drosophila* neurodevelopment assays. Using three fly mutant alleles of the *Drosophila* homologue *fzr* and overexpression studies, we show that patient variants can affect proper neurodevelopment.

With the recent report of a patient with neonatal-onset with microcephaly who also carries a *de novo FZR1* missense variant, our study consolidates the relationship between *FZR1* and developmental and epileptic encephalopathy and expands the associated phenotype. We conclude that heterozygous loss-of-function of *FZR1* leads to developmental and epileptic encephalopathies associated with a spectrum of neonatal to childhood-onset seizure types, developmental delay and mild ataxia. Microcephaly can be present but is not an essential feature of *FZR1*-encephalopathy. In summary, our approach of targeted sequencing using novel gene candidates and functional testing in *Drosophila* will help solve undiagnosed myoclonic atonic epilepsy or developmental and epileptic encephalopathy cases.

1 Department of Molecular and Human Genetics, Baylor College of Medicine, Houston, TX 77030, USA
2 Jan and Dan Duncan Neurological Research Institute, Texas Children's Hospital, Houston 77030, USA
3 Neurogenetics Group, VIB Centre for Molecular Neurology, Antwerp 2610, Belgium
4 Laboratory of Neurogenetics, Institute Born-Bunge, University of Antwerp, Antwerp 2610, Belgium

Received June 14, 2021. Revised September 21, 2021. Accepted October 18, 2021. Advance access publication November 11, 2021

5 Applied and Translational Neurogenomics Group, VIB Centre for Molecular Neurology, VIB, Antwerp 2610, Belgium
6 Center for Pediatric Neurological Disease Research, Department of Cell and Molecular Biology St. Jude Children's Research Hospital, Memphis, TN 30105, USA
7 Division of Child Neurology, Department of Paediatrics, Marmara University, Faculty of Medicine, Turkey
8 Child Neurology, AZ Delta, Roeselare, Belgium
9 Institute of Human Genetics, University Medical Centre Hamburg-Eppendorf, 20251 Hamburg, Germany
10 Department of Paediatrics, University Medical Centre Hamburg-Eppendorf, 20251 Hamburg, Germany
11 Department of Molecular Biology and Genetics, Bogazici University, Istanbul, Turkey
12 Department of Neurology, University Hospital Antwerp, Antwerp 2650, Belgium
13 Department of Neuroscience, Baylor College of Medicine, Houston, TX 77030, USA
14 Program in Developmental Biology, Baylor College of Medicine, Houston, TX 77030, USA
15 Development, Disease Models & Therapeutics Graduate Program, Baylor College of Medicine, Houston, TX 77030, USA
16 Translational Neurosciences, Faculty of Medicine and Health Science, University of Antwerp, Antwerp 2650, Belgium
17 μNEURO Research Centre of Excellence, University of Antwerp, Antwerp 2610, Belgium
18 Howard Hughes Medical Institute, Baylor College of Medicine, Houston, TX 77030, USA

Correspondence to: Sarah Weckhuysen
Professor, VIB-UAntwerp Centre for Molecular Neurology
Antwerp University Hospital, Antwerp, Belgium
E-mail: sarah.weckhuysen@uantwerpen.vib.be

Correspondence may also be addressed to: Hugo J. Bellen
Investigator, Howard Hughes Medical Institute, Distinguished Service Professor
Baylor College of Medicine, Houston, TX, USA
E-mail: hbellen@bcm.edu

Keywords: myoclonic atonic epilepsy; developmental and epileptic encephalopathy; *Drosophila* model of neurodevelopmental disorders; functional validation of novel variants; *FZR1*

Abbreviations: APC = anaphase promoting complex; ASD = anti-seizure drug; CADD = Combined Annotation Dependent Depletion; CLB = clobazam; DEE = developmental epileptic encephalopathy; EMS = ethyl methanesulphonate; ERG = electroretinogram; gnomAD = Genome Aggregation Database; HRP = horseradish peroxidase; LEV = levetiracetam; LTG = lamotrigine; MAE = myoclonic atonic epilepsy; MARCM = mosaic analysis with a repressible cell marker; VPA = valproic acid; WES = whole-exome sequence

Introduction

Developmental and epileptic encephalopathies (DEEs) are a heterogeneous group of disabling disorders, characterized by a combination of severe epilepsy and neurodevelopmental problems.[1] Seizures in DEE patients usually have an early age-of-onset and are often refractory to anti-seizure drugs (ASDs). The majority of DEE cases are thought to have a genetic basis, usually in the form of rare *de novo* variants with a highly disruptive effect on gene expression or protein function. Pathogenic variants in more than 100 genes have been associated with a DEE phenotype so far.[2–4] Identifying the causal variant in a DEE patient can bring an end to an often long and stressful diagnostic odyssey and may lead to improved or targeted treatment for a subset of the cases.[2,5,6]

We set out to identify novel variants in DEE patients by screening a large cohort of patients with myoclonic atonic epilepsy (MAE), a subtype of DEE, as part of the efforts of the EuroEPINOMICS-RES consortium.[7] MAE (previously known as myoclonic astatic epilepsy or Doose syndrome) is characterized by generalized seizure types including myoclonic, atonic, myoclonic-atonic, absence and tonic–clonic seizures. EEG typically shows generalized (poly)spike and waves and seizure onset is typically between 7 months and 6 years.[8] Using a combination approach of trio whole-exome sequencing (WES) and subsequent screening with a targeted gene panel including candidate genes for MAE, we identified two individuals diagnosed with MAE who each carried a unique *de novo* missense variant in *FZR1*. A third individual with a DEE with childhood-onset generalized epilepsy and a *de novo* missense variant was identified through GeneMatcher.[9]

FZR1 (fizzy and cell division cycle 20 related 1) encodes Cdh1, one of the two regulatory subunits of the anaphase-promoting complex (APC) that confers the substrate-specificity on this E3 ubiquitin ligase complex.[10] APC was initially identified to play a key role in mitotic cell cycle progression.[11] When Cdh1 associates with APC (Cdh1-APC), it controls mitotic exit leading to G1 arrest.[12] *Cdh1/Fzr1* knockout in mice leads to embryonic lethality, suggesting that this gene plays critical roles in development *in vivo* in mammals.[13] These *Fzr1* knockout mice, which die as embryos, have impaired cortical neurogenesis due to delay of mitotic exit, leading to reduced cortical size and thickness.[14] Cdh1-APC also has a prominent function in post-mitotic cells in the nervous system.[15] It controls neuronal survival,[16,17] axonal growth[18] and synapse formation and function.[19] Similar to its mammalian counterpart, the *Drosophila* homologue of *FZR1*, *fzr* (fizzy-related), has been studied in the context of neurodevelopment in addition

to its role in cell-cycle regulation as part of the APC.[18,20–22] *fzr* is necessary for photoreceptor patterning and regulates glial cell migration from the brain into the eye imaginal disc.[18] Through a forward genetic screen, we previously isolated two *fzr* alleles which displayed abnormal retina patterns and defects in electroretinograms (ERGs).[23] These phenotypes have been reported in hypomorphic mutants of *fzr*, which were first identified through their rough eyes, leading to one of the gene's synonyms 'retina aberrant in pattern (*rap*)'.[24] These previously generated *fzr* alleles provide genetic tools to test the functionality of the human *FZR1* variants identified in DEE patients.

During the course of our study, a different rare variant in *FZR1* was reported in an individual with microcephaly and DEE.[25] This study showed that the missense variant found in their patient led to decreased stability of the FZR1 protein in patient leucocytes and in HEK293T cells as well as accumulation of proteins targeted by Cdh1-APC.[25] The mutant protein was also unable to rescue the aberrant cell-cycle distribution of primary cortical progenitors from *Cdh1/Fzr1* knockout mice. Based on these data, the authors argued that this variant potentially contributes to microcephaly in the patient.

Here, we present three individuals with DEE and a novel *de novo* missense variant in *FZR1*. Two patient variants lead to the same amino acid change, and the third variant affects the same residue as affected in the previously published case.[25] These cases consolidate the role of *FZR1* in DEE and expand the phenotypic spectrum of *FZR1*-related encephalopathy to DEE with childhood-onset generalized epilepsy, mild ataxia and normal head circumference. To determine the functional consequence of the missense variants, we assessed the ability of the variant proteins to rescue the eye phenotype of the fly *fzr* mutant alleles isolated from a forward genetic screen using mosaic analysis. Furthermore, we also generated a new loss-of-function allele of *fzr* using the CRIMIC (CRISPR-Mediated Integration Cassette) technology[26] to study the impact of the patients' variants during development. Through these assays in *Drosophila*, we provide functional evidence for a loss-of-function mechanism of the pathogenic variants found in our patients, further supporting the involvement of FZR1 in DEE.

Materials and methods

Identification of patients with *de novo FZR1* variants

Patient 1 was recruited to the project on MAE of the EuroEPINOMICS-RES consortium.[7] WES was performed on an initial cohort of 39 parent–offspring trios (including Patient 1) with MAE at the Wellcome Trust Sanger Institute (Hinxton, Cambridgeshire). MAE was defined as the presence of myoclonic and (myoclonic–)atonic seizures and generalized (poly)spike waves on EEG in a child with previous normal or mildly delayed development. MRI of the brain should have excluded an acquired cause of the phenotype. WES and subsequent data analyses were performed as previously described.[27] Coding variants that lead to a missense change, stop gain/loss, frameshift or essential splicing change and were not present in the Exome Aggregation Consortium (ExAC)[28] and Genome Aggregation Database (gnomAD, v2.1.1)[29] with a frequency >0.01 or >0 for homozygous and X-chromosome or heterozygous variants, respectively, were retained. We also excluded variants in genes that are not expressed in the brain in the Genotype–Tissue Expression project database (V8).[30] Missense variants with a Combined Annotation Dependent Depletion score (CADD, v1.6)[31] <20 were excluded. All remaining candidate variants following a recessive, *de novo* or X-linked inheritance were validated using Sanger sequencing.

Patient 2 was part of a follow-up cohort consisting of 211 DEE patients, including 89 probands with MAE and 122 probands with Dravet or Dravet-like syndrome. The cohort was screened using a targeted gene panel using Molecular Inversion Probes and consisted of the coding regions of 12 known and 40 candidate genes (at time of screening) for MAE, including *FZR1* (Supplementary Table 1). Candidate genes included in this panel were selected from a list of genes with single *de novo* hits identified in the EuroEPINOMICS-RES WES data. Data analysis and variant filtering was performed as previously described.[32] Segregation analysis was performed using Sanger sequencing for all non-synonymous, frameshift and splice-site variants that were not present in the ExAC set of ~61,000 WES.[28] Paternity and maternity were confirmed using the Powerplex®16S system (Promega).

Patient 3 was identified through GeneMatcher.[33] Trio-WES was performed in a clinical diagnostic setting using DNA from the patient and both healthy parents. Trio-exome data were filtered for non-synonymous *de novo* variants absent in the general population (gnomAD) and for rare biallelic variants with minor allele frequency $<0.1\%$ and absence of homozygous carriers in the aforementioned database. The functional impact of the identified missense variants was predicted using the CADD v1.6,[31] SIFT (Sorting Intolerant from Tolerant)[34] and Polyphen[35] pathogenicity prediction tools.

The Ethical Committees of all local institutes participating in EuroEPINOMICS-RES approved the study. Parents of each patient signed an informed consent form for participation in the study.

Drosophila reagents for analysis of DEE variants

The molecular lesions of two ethyl methanesulphonate (EMS)-induced variants identified from our previous forward genetic screen,[23] fzr^{A} and fzr^{B}, were identified using Sanger sequencing of PCR amplicons of genomic DNA.[36] ERG analyses on mosaic adult eye were performed as described earlier.[37] The generation of the CRIMIC allele, *Drosophila* overexpression stocks for wild-type and variant-carrying cDNAs, the details of characterization of these alleles and crosses used to perform the mosaic analysis with a repressible cell marker (MARCM) analysis are provided in the online Supplementary material.

Genotype to phenotype association analysis

Excess *de novo* variant presence in DEE patients for FZR1 was evaluated using denovolyzeR.[38] For this analysis we used the two *de novo* missense variants identified in the combined research cohort of 250 patients examined in our study. In parallel, we determined the number of rare, potentially damaging variants in *FZR1* in the control population set of gnomAD[28] based on CADD,[31] SIFT[34] and Polyphen[35] scores using the Variant Effect Predictor tool from Ensembl.[39] We filtered missense variants and loss-of-function variants that had a general population frequency of less than or equal to 0.01, had a CADD score greater than or equal to 20 and were predicted to be Pathogenic/Likely pathogenic by SIFT and Polyphen. For this analysis segregation of variants was ignored. We performed a chi-square test to evaluate the allele-count excess as well as number of unique variant preponderance in the DEE patient cohorts compared to the gnomAD (control) population.

Evaluation of relative positions of affected residues in the 3D structural model of human Cdh1

To examine the localization of the residues predicted to be altered by the patients' missense variants, we used the 3D structural model of Cdh1 generated from an electron microscopy

reconstruction of the *Homo sapiens* APC (PDB ID: 4ui9).[9] We used PyMOL (Molecular Graphics System, Version 2.0 Schrödinger, LLC) to map the location of the residues affected. We also predicted the location of the *Drosophila* Fzr^{A} variant based on the homology of human FZR1 and *Drosophila* Fzr proteins (Supplementary Fig. 2A).

Electroretinogram analysis of adult mosaic eyes

y w fzr^{B}, *FRT19A/FM7c*, *Kr-GAL4*, *UAS-GFP* and *y w* fzr^{A}, *FRT19A/FM7c*, *Kr-GAL4*, *UAS-GFP* (BDSC 52384) females were crossed with *y w FRT19A; ey-FLP* (BDSC 5579). The resulting females carried mosaic eyes with mutants identifiable with the lack of red pigmentation. ERG analyses on mosaics were performed as described earlier.[23,37]

Immunofluorescence analysis of *Drosophila* tissue

Immunofluorescence analysis was performed as described earlier on embryos and third instar larval eye imaginal discs.[18,20] Samples were imaged using a LSM 500 confocal microscope (Zeiss) to generate a Z-stack of different focal planes. The confocal Z-stack images were used to generate maximum intensity Z-projection using ImageJ.[40]

In vitro overexpression analysis of DEE-associated variants

Human *FZR1* cDNA (NM_001136198.1) in the donor vector pDONR221 (HsCD00042756;) was purchased from Harvard cDNA clone repository. The coding region was cloned into the pEzy-eGFP (Addgene #18671) destination vector in frame with an N-terminal eGFP tag using Gateway™ LR Clonase™ II Enzyme mix (ThermoFisher 11791020) following the manufacturer's recommended protocol. The variants observed in the DEE patients were introduced into the pEzy-eGFP-FZR1 using Quickchange II site directed mutagenesis kit (Agilent).

Data availability

All WES data generated in the EuroEPINOMICS-RES project were deposited in the European Genome–Phenome Archive, accession numbers EGAS00001000190, EGAS00001000386 and EGAS00001000048.

Results

Clinical case reports

Patient 1 is a 17-year-old male born at term in a non-consanguineous family of Turkish origin. He had an elder brother with mild learning disabilities without epilepsy and a paternal grandmother with lesional epilepsy. At the age of 3 years and 11 months the proband presented at the paediatric neurology clinic with generalized tonic–clonic seizures. Some developmental delay had already been noticed prior to seizure onset and mainly manifested as delay in receptive and expressive language development and fine motor skills. At the age of 4 years and 2 months, he developed myoclonic and atonic seizures and at 4.5 years of age absences were noted. The patient was first treated with valproic acid (VPA), which decreased the seizure frequency and duration but led to continuation of frequent drop attacks. He was subsequently treated with levetiracetam (LEV), clobazam (CLB) and lamotrigine (LTG). He eventually became seizure-free at 4.5 years on a combination of CLB and VPA. EEG at 4 years of age showed a slow background and generalized epileptic activity. A sleep EEG at the age of 4 years demonstrated frequent generalized spike waves (Supplementary Fig. 1A). Multiple EEGs at ages 6–7 years were normal. EEGs at 8 and 11 years showed rare epileptic discharges, both focal and generalized, but no clinical recurrence of seizures was noted. On clinical examination the boy had a mild ataxic gait and some orofacial coordination problems. He spoke a few words, and there were no evident dysmorphic features. Head circumference was at the 23rd percentile (54 cm at 17 years). The patient was diagnosed with MAE with moderate intellectual disability. Currently, there are mild behavioural problems (hyperactivity and attention problems), but he is very social.

Patient 2 is a 14-year-old female, born at 42 weeks gestational age in a non-consanguineous family of Moroccan origin. There was no known history of epilepsy or developmental delay in this family. She has one healthy younger brother. The neonatal period was unremarkable. Early motor milestones were marginally normal: she sat up straight at the age of 9 months and walked at the age of 18 months. A delay in language development and an instable gait were noticed at the age of 2.5 years. At the age of 2 years and 10 months she had a developmental index lower than 55 on the Bayley II developmental scale, correlating with a developmental age of 16 months. On clinical examination a moderate crouch gait and hyporeflexia were observed. Seizures first started at 3.5 years of age, with more than 10 generalized tonic–clonic seizures a day. Later, the patient developed myoclonic, tonic, tonic–clonic, atonic seizures and atypical absences. Multiple EEGs showed generalized epileptic activity (Supplementary Fig. 1B). Initial treatment with VPA had a temporary effect on seizure frequency. Add-on of LEV induced a new seizure type characterized by upward eye deviation, head drop and sometimes falling, after which LEV was stopped. Further treatment with combinations of ASD including nitrazepam, CLB, topiramate, LTG, carbamazepine, ethosuximide, felbamate, sulthiame and vagal nerve stimulation all had little effect on seizure frequency. She currently still has daily atypical absences and rare tonic–clonic seizures. Metabolic screening, examination of CSF and skin biopsy were normal. On brain MRI at the age of 2.5 and 3.5 years of age, subtle white matter lesions were observed periventricular and in the parieto-occipital lobes (Supplementary Fig. 1E), thought to reflect delayed myelination. Last MRI at age 8 showed an almost complete normalization of the imaging abnormalities (Supplementary Fig. 1F and G). At last follow-up, she speaks a few isolated words, has a mild ataxic gait and a severe intellectual disability. Other comorbidities are autism spectrum disorder and behavioural and concentration problems.

Patient 3 is a 3-year-old female, the first child of healthy consanguineous parents from Afghanistan. She has a healthy 2-year-old sister. She was born after an inconspicuous pregnancy at 40 + 4 weeks of gestation. The birth measurements were normal [birth weight 3620 g (–0.2z), birth length 52 cm (0z), occipitofrontal circumference at birth 36 cm (0.7z)]. The neonatal period was unremarkable except for an oozing navel. A muscular hypotonia was noticed at the age of 5 months. Milestones of motor development were reached delayed: she sat up straight at the age of 14 months and started walking at the age of 26 months. Language development was delayed as well: at 3 years she only speaks a few words; receptive language is less impaired. Cognitive development is also not age-appropriate. Clinical examination at the age of 2 years showed a muscular hypotonia, coordination problems and an ataxic gait. A sleep EEG at the age of 1.5 years showed generalized spike-wave paroxysms. Seizures started at the age of 2 years and 9 months and consisted of generalized tonic–clonic seizures. After initial therapy with LEV she was seizure-free for 1.5 months. Soon, and despite addition of CLB, generalized tonic–clonic seizures recurred every 2 weeks. A probationary treatment with valproate was not tolerated. After her third birthday, there was an increase in seizure frequency with several serial seizures a day. Seizures

consisted of starred gaze with myoclonic jerks of the arms and smiling and frequent generalized tonic–clonic seizures. Therapy with LEV was replaced by lacosamide and LTG. EEG at 3 years of age showed a slow background and bursts of generalized sharp waves and irregular slow spike-wave activity (Supplementary Fig. 1C and D). Brain MRI revealed a mild frontotemporal accentuated volume reduction and bilateral white matter hyperintensities suggestive of delayed or hypomyelination (Supplementary Fig. 1H-J). Because of difficulties in taking her medication, she received a percutaneous endoscopic gastrostomy tube at age 3 years 4 months.

A summary of the clinical history of the three patients described above, and the patient described by Rodriguez *et al.*,[25] can be found in Table 1.

Genetic diagnosis

WES on Patient 1 and unaffected parents yielded a *de novo* missense variant in *FZR1* [c.559G>A, p.(D187N), Table 1] located at the same residue as the previously reported *de novo* missense variant in a patient with microcephaly, psychomotor retardation and epilepsy [p.(D187G)].[25] No other variants passed the filtering steps as described in the 'Materials and methods' section. An elder brother with mild learning disabilities but no seizures did not carry the variant. The variant is not present in the gnomAD database (v2 and v3) and has a CADD score of 29.7,[31] a SIFT score of 0.01[34] and a PolyPhen score of 0.936,[35] all indicating a deleterious or probably damaging effect. The variant was also absent from the NDAL inhouse database (Koç University-KUTTAM, İstanbul, Turkey), including 2282 exomes of Turkish patients with various neurological disorders or diabetes/obesity and 803 genomes from Turkish amyotrophic lateral sclerosis patients and healthy controls. According to the gnomAD database,[29] *FZR1* has a pLI score of 1, observed/expected score of 0.04, and a z-score of 3.64 for missense variants, showing that this gene is intolerant to both loss-of-function (nonsense, frameshift, core splicing) and missense variants.

Following the identification of a *de novo FZR1* missense variant in Patient 1, a follow-up panel-screening resulted in the identification of another *de novo FZR1* missense variant [c.999C>G, p.(N333K), Table 1] in Patient 2. This variant had a CADD score of 23.6, a SIFT score of 0.01 and a PolyPhen score of 0.814, all predicting a deleterious or possibly damaging effect. This variant was also absent from the gnomAD database. Previous genetic tests on this patient included karyotype analysis and *SCN1A* and *PCDH19* screening, all of which were negative. Array-based comparative genomic hybridization (array-CGH) showed two duplications on Chr11p11.2. These copy number variations were inherited from the healthy mother and did not include disease-associated genes. Therefore, they were deemed non-contributing to the patient phenotype.

Patient 3 was identified through GeneMatcher, and carries a *de novo* missense variant at the same nucleotide position as Patient 2, leading to an identical amino acid change [c.999C>A, p.(N333K), Table 1], with identical CADD, SIFT and PolyPhen scores. Previous chromosome analysis and array-CGH were normal. Filtering of exome data retained homozygous variants in two additional genes, not yet reported in the context of rare Mendelian disorders. The missense variant c.2105_2106delinsTC, p.(S702F) in *PTPN21* (NM_007039.4) had a SIFT score of 0.000 and a PolyPhen score of 0.996, predicting a probably damaging effect. This multi-nucleotide variant is present twice heterozygous in gnomAD. PTPN21 (tyrosine-protein phosphatase non-receptor type 21) is an oncogenic protein known to be upregulated in several types of cancer cells[41] and functions as a key regulator of inflammation.[42] Two non-synonymous single-nucleotide polymorphisms in PTPN21 showed association to schizophrenia in a genome-wide association study.[43] In neurons, PTPN21 controls the activity of KIF1C, a fast organelle transporter implicated in the transport of dense core vesicles and the delivery of integrins to cell adhesions.[44] It was further shown to positively influence cortical neuronal survival and to enhance neuritic length.[45] The second homozygous variant identified in Patient 3 was the truncating variant c.577C>T, p.(R193*) in the last exon of *TPD52L2* (NM_199360.3). TPD52L2 (tumour protein D52-like 2) is a ubiquitously expressed tumour protein shown to be involved in multiple membrane trafficking pathways and to affect cell proliferation, adhesion and invasion.[46,47] As the *de novo FZR1* missense variant resulted in the same amino-acid substitution as identified in Patient 2 who has a very similar phenotype, we concluded that the *FZR1* variant is most likely to underlie the neurological disease of Patient 3. We cannot, however, totally exclude the possibility that the variants in *PTPN21* and *TPD52L2* contribute to the phenotype of Patient 3.

Having found these cases, we tested the association between rare variants in *FZR1* and DEE using two different genetic association testing tools. First, we used the tool denovolyzeR,[38] which evaluates the overrepresentation of *de novo* variants that affect the protein sequence (missense and loss of function variants) in a specific gene. We found that identification of two *de novo* variants in *FZR1* amongst the 250 patients in our research cohort is a 212-fold enrichment (Poisson distribution *P*-value of 4.41e-05) over the expected number of *de novo* variants, suggesting a strong association of *FZR1 de novo* missense variants with the disorder. Second, we compared the rate of rare, damaging variants in our research cohort (250 patients) with that of general population in gnomAD (141 456 samples)[29] in *FZR1*. Once again, we found a significant enrichment in the number of damaging variants in *FZR1* within our patient cohort (2/250 patients) compared to that of gnomAD (total allele count = 97, unique variants = 57; chi-square test *P*-value for unique variants = 1.613e-05; chi-square test *P*-value for total allele count = 0.001574).

DEE-associated *FZR1* variants lead to reduced protein abundance

FZR1 and its homologues in other species are highly conserved, with *Drosophila fzr* protein showing over 70.3% identity (79% similarity) with human FZR1. The amino acids that are impacted by the missense variants that we identified in the patients are conserved in *Drosophila fzr* (Fig. 1A and Supplementary Fig. 2A). To test the effect of the patient variants on protein stability and localization, we expressed FZR1 with an N-terminal eGFP tag in HEK293 cells. FZR1 expression was detected in the nucleus, with a weaker diffuse signal in the cytoplasm (Fig. 1B). Variant FZR1 proteins showed a similar pattern of localization. However, western blot of total protein from cells transfected with wild-type or mutant eGFP-FZR1 showed a clear difference in FZR1 abundance, with both patient variants leading to a reduction in protein level of approximately 40% ($P < 0.01$; Fig. 1C and D).

To further examine the effect of patient variants on human FZR1 function, we mapped the affected residues in a 3D protein structure of the APC.[10] Variants found in all three patients affect residues within the WD40 domain of the FZR1 protein (Fig. 1E and F and Supplementary Fig. 2B). WD40 domains, also known as beta-transducing repeats, enable protein–protein interactions,[48] and *de novo* variants in another WD40 repeat containing protein encoding gene *WDR37* have also been recently associated with epilepsy.[49] The active site of a WD40 domain is often found in the central cleft of the propeller where the loops connect the successive beta sheets. As both variants are present in those loops (Fig. 1E and F),

Table 1 Clinical features

	Patient 1	Patient 2	Patient 3	Rodriquez *et al.*[25]
Sex	Male	Female	Female	Male
Age at study	17 years	15 years	3 years	4 years
Ethnic origin	Turkish	Moroccan	Afghan	Spanish
FZR1 variant (NC_000019.9, NM_016263.3)	g.3527717G>A c.559G>A, p.(D187N)	g.3532084C>G c.999C>G, p.(N333K)	g.3532084C>A c.999C>A, p.(N333K)	g.3527718A>G c.560A>G, p.(D187G)
Inheritance	*De novo*	*De novo*	*De novo*	*De novo*
Development prior to seizure onset	Delayed language development, fine motor problems	Delayed language development, instable gait	Delayed motor and language development	NA (neonatal sz)
Age at seizure onset	3 years 11 months	3 years 6 months	2 years 9 months	Neonatal
Type(s) of seizure at onset	Generalized tonic clonic sz	Generalized tonic clonic sz	Generalized tonic clonic sz	Right hemiclonic sz
Additional seizure types	Myoclonic, atonic, absences	Myoclonic, tonic, atonic, atypical absences	Myoclonic, atypical absences	Right and left hemiclonic, left focal, versive, generalized tonic–clonic
EEG at onset	Slow background, generalized epileptic activity	Slow background, burst of high-voltage slow waves	Generalized spike-wave complexes	NA
Later EEG studies	Normal or rare focal or generalized epileptic discharges	Slow background. Further normal or rare generalized epileptic discharges	Slow background. Generalized sharp waves and irregular slow spike-wave complexes	Ictal EEG: sz origin from right and left hemisphere with continuous migratory ictal foci
ASDs trialled	VPA, LEV, CLB, LTG	VPA, LEV, NTZ, CLB, TPM, LTG, CBZ, ETX, FLB, SLT	LEV, CLB, VPA, LCS, LTG	VPA, LEV, RUF, CLZ, VIG, TPM, KETO
Current ASDs	VPA, CLB	VPA, CLB, LTG, SLT, VNS	CLB, LTG	NA
Drug-resistant	No. Sz free at age 4.5 years on current ASD combination	Yes	Yes	Yes
Intellectual disability	Moderate	Severe	Severe	Profound
Behavioural problems	Hyperactivity and attention problems	ASD, attention problems	No	NA
Brain MRI	Normal	Aspecific parieto-occipital white matter hyperintensities (at 2.5 and 3.5 years)	Mild frontotemporal accentuated volume reduction; FLAIR hyperintense signal alterations paratrigonal to frontoparietal (3 years)	Microcephaly, further normal
Head circumference (age) [percentile]	54 cm (17 years) [23rd]	52.8 cm (14 years) [4th]	49 cm (3 years) [42nd]	47 (4 years) [<3rd]
Neurological exam	Mild ataxic gait and some orofacial coordination problems	Moderate crouch gait, lumbar hyperlordosis, hyporeflexia, mild ataxic gait	Muscular hypotonia, coordination problems, mild ataxic gait	Severe axial hypotonia, exaggerated deep-tendon reflexes, spasticity
Other features	No	No	Dysmorphic features: deep-set eyes, high nalas bridge, broad nasal tip. Low set ears. Sleep disturbance	Cardiac ultrasound: mild mitral and tricuspid insufficiency and left ventricular hypertrophy
Epilepsy syndrome	MAE	MAE	Not further specified DEE	EIMFS

CBZ = carbamazepine; CLZ = clonazepam; EIFMS = epilepsy of infancy with migrating focal seizures; ETX = ethosuximide; FLB = felbamate; KETO = ketogenic diet; LCS = lacosamide; NA = not applicable; NTZ = nitrazepam; RUF = rufinamide; SLT = sulthiame; sz; seizures; TPM = topiramate; VIG = vigabatrine; VNS = vagal nerve stimulation.

they may interfere with the protein–protein interaction sites and potentially affect the substrate binding capacity of FZR1 in addition to reducing overall protein stability.

Genetic characterization of *fzr* alleles in *Drosophila*

We decided to examine the functional effect of the DEE-associated variants that we identified using *Drosophila* as a model organism. For this study we used two EMS-induced alleles of *fzr* (fzr^{A} and fzr^{B}) that we previously isolated. These alleles produce rough eye phenotypes in adult mosaic animals and show defects in ERGs,[23] suggesting that *fzr* is involved in the development and function of the fly visual system. We determined the molecular lesions in these lines using Sanger sequencing of PCR fragments of genomic DNA. The molecular lesions in the fzr^{A} allele is a canonical splice-site mutation (fzr-RA: c.592+1G>A) and the fzr^{B} allele is a missense

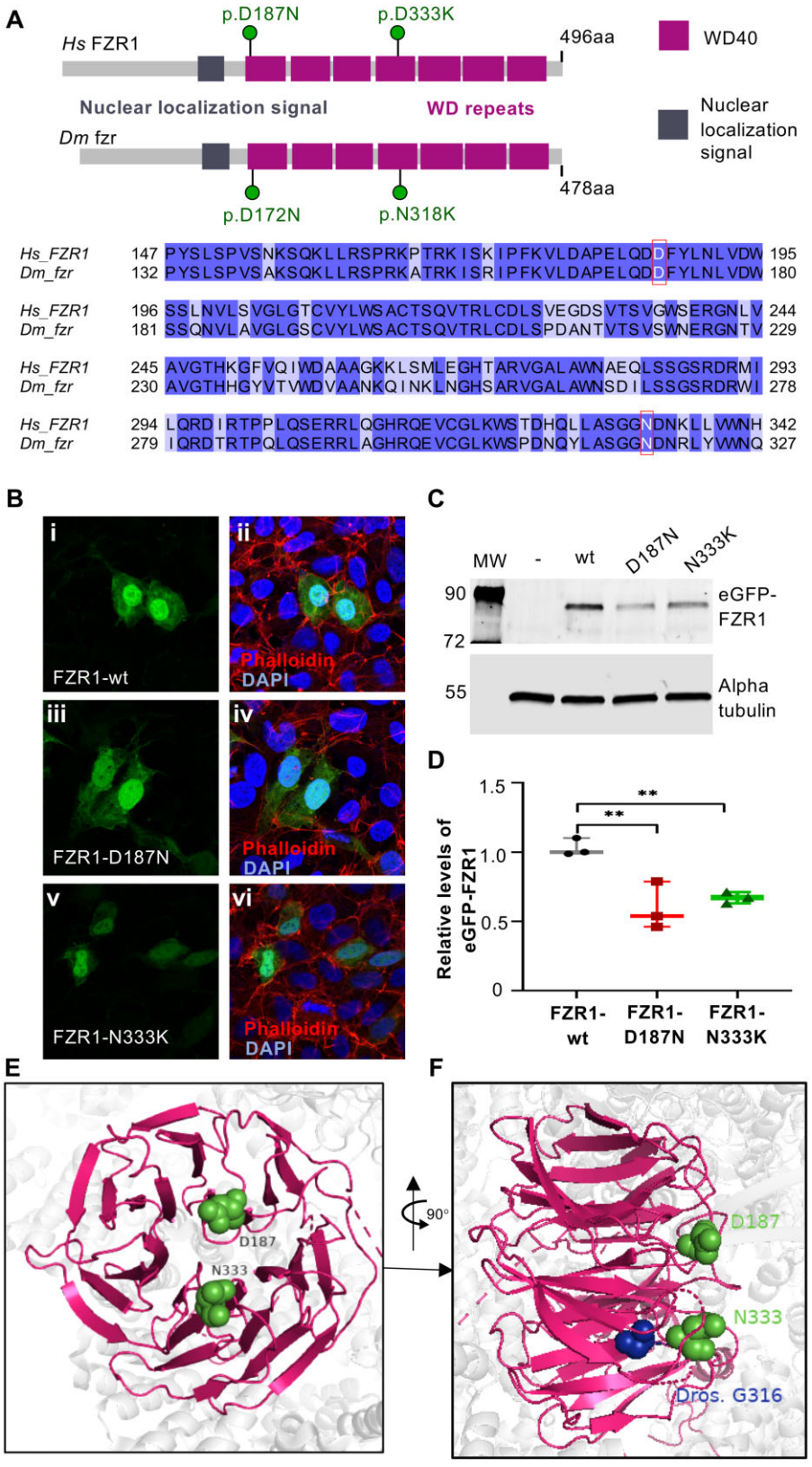

Figure 1 Conservation FZR1 and *in vitro* analysis of DEE variants in mammalian cells. (**A**) Protein primary structure diagram of human FZR1 and *Drosophila* orthologue Fzr showing conserved domains and corresponding positions of variants observed in patients. The residues affected in the patients are conserved in *Drosophila melanogaster*. Amino acid sequence alignment of human FZR1 and *Drosophila fzr* region encompassing the DEE variant residues, which are shown in red boxes. (**B**) Immunofluorescence staining for eGFP-tagged human FZR1 cDNA in HEK293 cells (green), co-stained with DAPI (nucleus; blue) and actin-cytoskeleton (Phalloidin; magenta). (**i–ii**) FZR1-wt, (**iii–iv**) FZR1:p.D187N, (**v–vi**) FZR1:p.N333K localization to the nucleus and the cytoplasm. (**C**) Western blot showing relative expression of FZR1-wt and variants in HEK-293 cells. Alpha-tubulin is used as loading control. (**D**) Box-and-whisker plot showing the quantitation of normalized western blot signal analysed using one-way ANOVA, followed by

(Continued)

mutation (fzr-PA: p.G316N; Fig. 2A). In the protein structure model, this fly mutation is found close to the p.N333K residue affected in Patients 2 and 3 (Fig. 1F).

We created an additional fly mutant by using CRISPR/Cas9 and homology directed repair to introduce an artificial exon containing a splice acceptor-T2A-GAL4-polyA cassette between the first and second exons of *Drosophila fzr*. This allele is predicted to generate a strong loss-of-function allele that also produces a GAL4 in the same spatial and temporal pattern reflecting the endogenous *fzr* expression pattern.[26] This CRIMIC insertion ($fzr^{CR00643\text{-}TG4.2}$, henceforth called $fzr^{T2A\text{-}GAL4}$) leads to precocious termination of transcription of all *fzr* isoforms because of the presence of a polyA termination signal as well as an interruption of translation of *fzr* mRNA due to the viral T2A peptide sequence. T2A also allows reinitiation of translation to express the GAL4 when and where endogenous *fzr* is expressed (Fig. 2A). The $fzr^{T2A\text{-}GAL4}$ allele permits expression of transgenes including *fzr* cDNA in the native pattern of *fzr* in the *fzr*-mutant background by crossing this line to a *UAS-fzr* transgenic fly (Fig. 2A),[26] simplifying the functional studies of the variants of interest.

We found that the $fzr^{T2A\text{-}GAL4}$ allele is recessive lethal and fails to complement the lethality of a previously reported null allele of *fzr* ($fzr^{ie}28$), suggesting that $fzr^{T2A\text{-}GAL4}$ is a strong loss-of-function allele (Fig. 2B). Complementation test between the $fzr^{T2A\text{-}GAL4}$ and the EMS-induced mutations (fzr^{A} and fzr^{B}) reaffirmed that these mutations are allelic and are also loss-of-function mutations (Fig. 2B). Finally, we examined the rescue of the recessive lethality of $fzr^{T2A\text{-}GAL4}$ and the EMS alleles using a duplication containing the *fzr* locus inserted on the third chromosome [*Dp(1;3)DC472*, *Dup*]. Each allele was individually rescued by this duplication and the rescued animals did not exhibit any morphological defects, confirming that the phenotypes observed in these alleles are due to loss-of-function of *fzr* (Fig. 2B). To examine the expression pattern of *fzr in vivo*, we crossed the $fzr^{T2A\text{-}GAL4}$ allele to a *UAS-nls::RFP* transgenic line and explored the fluorescent pattern. We found that *fzr* is broadly expressed in larval brains and eye imaginal discs, consistent with their developmental roles in these tissues (Fig. 2C and D).

The role of *fzr* in neurodevelopment in embryos and larva

To further characterize the phenotypes of the *fzr* alleles we generated, we first examined the effect of the *Drosophila* EMS mutants in developing larval eye imaginal disc and adult retina. We tracked the stereotypical pattern of larval photoreceptor precursors in homozygous mutant cells induced through the expression of *eyeless* (*ey*) enhancer driven flippase[50] (*ey-FLP*) that is generated using the MARCM technique.[51] In this experiment, flippase mediates the recombination of two FRT (flippase recognition target) sites located at the base of the X-chromosome (FRT19A). When this occurs during mitosis and one of the two sister chromatids carries the *frz* mutant allele, homozygous mutant and homozygous wild-type cells are generated from heterozygous cells (Fig. 3A). Simultaneously, it reverses the repression of GAL4 by GAL80 in homozygous mutant cells, allowing the GAL4 to drive the expression of a GFP reporter and simultaneously an optional *UAS-fzr cDNA* transgene (wild-type or variant, Fig. 3B). Consequently, mutant cells are marked by the GFP reporter and if included, transgenes are expressed within these mutant cells to rescue the phenotype caused by *fzr* loss-of-function.

In the larval eye disc, the developing photoreceptors were marked by staining for ELAV (embryonic lethal abnormal vision), a pan-neuronal nuclear marker.[52] In the homozygous mutant cells identified using GFP reporter, we found that the larval photoreceptor patterns marked by ELAV were severely affected (Fig. 3C). This phenotype in the fzr^{B} allele is consistent with previous reports of *fzr* function in the eye.[18] In adults the pattern of the compound eye was also significantly affected in animals in which mutant mosaic clones were generated (Fig. 3D).

To further assess the function of photoreceptors, we performed ERG recordings on 3–4-day-old flies. Adult flies with *fzr* mosaic eyes showed a significant reduction in the depolarization amplitude of the ERG response to light (Supplementary Fig. 3A and B), indicating a defect in phototransduction. These flies also showed severe loss of the ON/OFF transients (Supplementary Fig. 3A and B), suggesting a defect in synaptic transmission.

Next, we examined the embryonic neurogenesis phenotype of the $fzr^{T2A\text{-}GAL4}$ mutants by assessing the morphology of the nervous system through immunofluorescence staining and confocal microscopy using an antibody that recognizes neuronal/photoreceptor membranes [anti-horseradish peroxidase (HRP) antibody]. Hemizygous $fzr^{T2A\text{-}GAL4}$ mutant males showed a clear defect in neuronal patterning in the CNS of fly embryos, displaying defective neuromere patterns in the ventral nerve chord (Supplementary Fig. 3C). This is consistent with the role of *fzr* in neuronal development and phenotypes reported for previously identified *fzr* alleles.[20]

DEE-associated variants fail to support *Drosophila* neurodevelopment in rescue experiments *in vivo*

fzr^{B} mosaic flies showed severe morphological defects in larval eye imaginal discs as evidenced from aberrant anti-HRP staining pattern in the mutant mosaic clones (Fig. 3E). We examined the ability of the *fzr* cDNA with wild-type sequence or cDNAs with variants corresponding to those of the human patients (Fig. 1A) to rescue this phenotype (MARCM).[53] We observed that overexpression of the wild-type fly fzr cDNA in the mutant mosaic clones rescued the HRP pattern defects in the eye discs [Fig. 3E(iii)], but the variant cDNAs failed to display a similar rescue [Fig. 3E(iv and v)]. *fzr* mutants in *Drosophila* have also been reported to exhibit defects in glial cell migration.[18] Because glia are known to play important roles in epilepsy,[54] we examined the impact of the two patient variants on this phenotype, again using the MARCM system in the eye imaginal disc. In a control animal [mosaic animals without *fzr* mutant tissue, Fig. 3E(i)], glial cells only migrate to areas where photoreceptors have initiated their differentiation program indicated by HRP-positive cells [Fig. 3E(i)]. However, in mosaic cells that are defective for *fzr*, we observed that glial cells migrate beyond the differentiated zone and prematurely enter areas where immature photoreceptors are present [HRP negative region, Fig. 3E(ii)]. We observed that wt *fzr* cDNA was able to suppress this phenotype [Fig. 3E(iii)] but the *fzr* cDNAs carrying the patient's variants were not able to rescue the abnormal migration of glial cells [Fig. 3E(iv

Figure 1 Continued
Dunnett's test for comparison of the variants to the wild-type expression. **Multiplicity adjusted *P*-value < 0.01. Boxes are drawn from the 25th to the 75th percentiles, with a line indicating mean, and error bars from maximum to minimum values. (**E** and **F**) 3D structural model FZR1 as part of the Cdh1-APC (PDB: 4ui9)[9] showing the relative positions of the variants affected in the DEE patients (green) and corresponding residue of the *Drosophila* mutation observed in the fzr^{B} allele (blue).

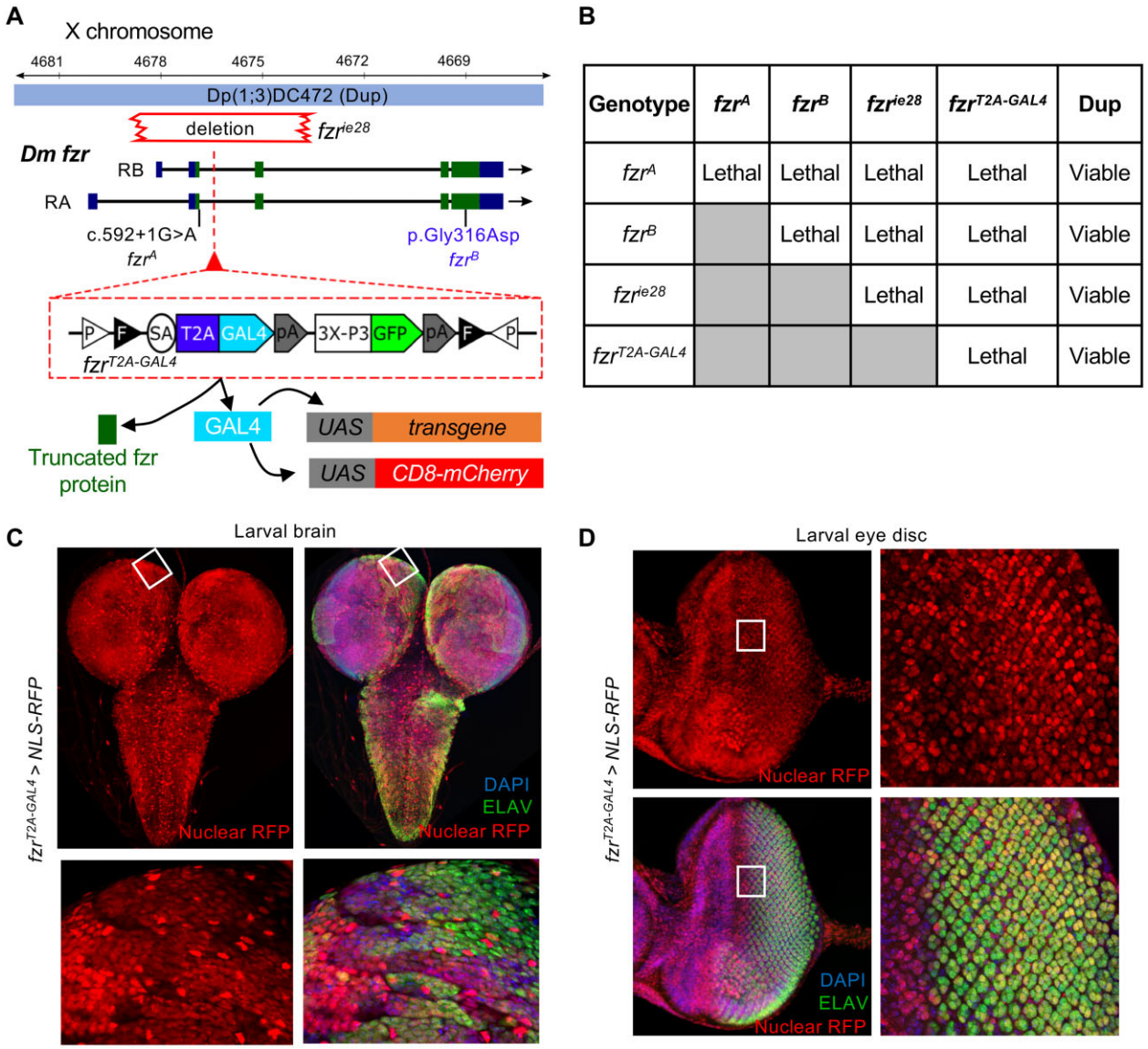

Genotype	fzr^{A}	fzr^{B}	fzr^{ie28}	$fzr^{T2A\text{-}GAL4}$	Dup
fzr^{A}	Lethal	Lethal	Lethal	Lethal	Viable
fzr^{B}		Lethal	Lethal	Lethal	Viable
fzr^{ie28}			Lethal	Lethal	Viable
$fzr^{T2A\text{-}GAL4}$				Lethal	Viable

Figure 2 *Drosophila fzr* alleles and expression pattern. (**A**) *Drosophila* X-chromosome locus showing two transcriptional isoforms of *fzr*, two EMS-induced mutation alleles fzr^{A} (splice-site mutation) and fzr^{B} (missense mutation located in the same domain as one of the patient's variants), fzr^{ie28} (deletion spanning the first two exons of *fzr*) and a third chromosome duplication allele carrying a complete copy of *fzr* from the X-chromosome. Also shown is the $fzr^{T2A\text{-}GAL4}$ allele generated by insertion of a mutagenic T2A-GAL4 artificial exon within the second intron of *fzr*. This insertion leads to termination of *fzr* translation and expression of GAL4 protein from the endogenous *fzr* locus. (**B**) Table showing results of complementation tests between various alleles of *fzr* as well the *fzr* locus duplication shown in **A**. (**C** and **D**) Expression pattern of fzr in *Drosophila* third instar visualized using the $fzr^{T2A\text{-}GAL4}$ driving the expression of *nls::RFP* (red) co-stained with ELAV marking neuronal cells (green) and DAPI to detect nucleus (blue). (**C**) Larval brain and higher magnification images of the boxed region. (**D**) The eye-antennal disc and higher magnification images of the boxed region.

and v)]. This suggests that neuron–glia communication mediated by *fzr* are also affected by the patient variants.

Because we noticed that overexpression of *fzr* wild-type cDNA in the eye clones occasionally led to aberrant development patterns, we examined whether overexpression of *fzr* cDNA in wild-type background can disrupt the normal photoreceptor development pattern. Indeed, when wild-type *fzr* cDNA was overexpressed in the developing eye using *ey-GAL4*, we observed a severe reduction in the size of adult retina and loss of photoreceptor pattern (Fig. 4A and B), similar to what has been reported earlier.[22] In this assay, we observed that *fzr* cDNA with patient variants also caused aberrant photoreceptor patterns (Fig. 4C and D). However, the reduction in the size of the adult retina due to the *fzr* variant overexpression was not as severe as the *fzr* wild-type cDNA and the differences between the overexpression of wild-type and variants were statistically significant (Fig. 4E). These results further support that *FZR1* variants associated with DEE are loss-of-function alleles.

We next examined if wild-type *UAS-fzr cDNA* can rescue the lethality observed in $fzr^{T2A\text{-}GAL4}$ flies. We used GAL4 expressed from the T2A-GAL4 allele to drive the expression of the *UAS-fzr*. Expression of wild-type *fzr* cDNA was able to allow a significant fraction (~20–23%) of $fzr^{-T2A\text{-}GAL4}$ hemizygous males to live to third instar larval stages, whereas they otherwise die as embryo or first instar larvae (Fig. 5A). In contrast, the overexpression of *fzr* cDNA carrying either of the two patient variants fails to rescue this early

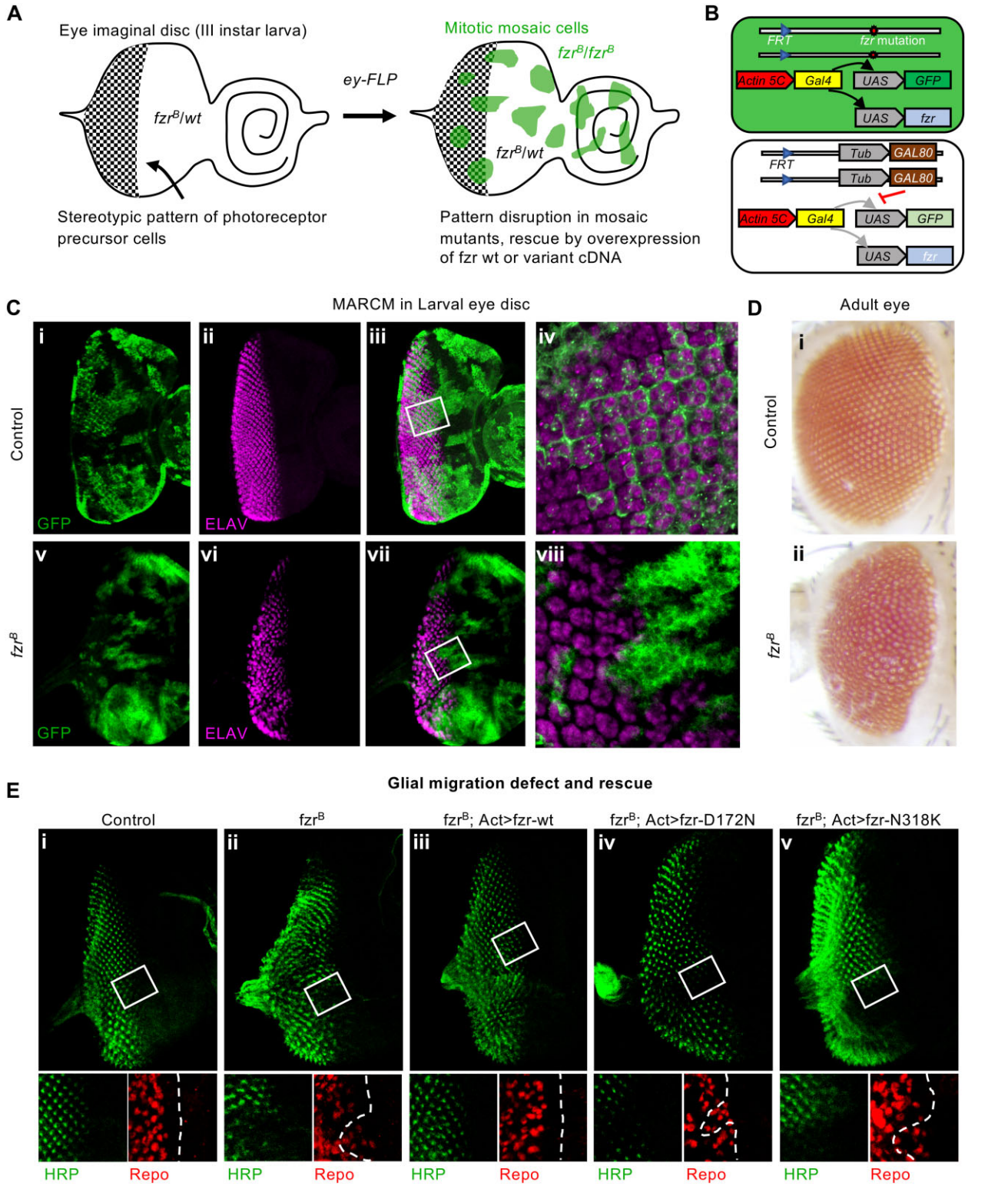

Figure 3 Pattern formation and glial migration defects in the photoreceptor precursors of *fzr* mutants are not rescued by DEE variants. (**A**) Diagram showing the generation of random mosaic patches of homozygous *fzr* mutant cells in the developing eye disc that are marked by GFP expression using MARCM. (**B**) Schematic diagram showing gene expression differences between homozygous *fzr* mutant (GFP+) cells and the surrounding heterozygous *fzr* (GFP–) cells. In mutant cells, *Actin5c-GAL4* drives the expression of GFP and *fzr* cDNA (wild-type or patient variant), while in heterozygous cells, GAL4 activity is suppressed by GAL80. [**C(i–iv)**] Control larval eye discs showing expression pattern of ELAV (red) in mosaics marked by GFP expression generated using MARCM. [**C(v–viii)**] Larval eye disc showing mosaic homozygous fzr^B tissue (green) showing dramatic change in ELAV (magenta) expression within and outside the clones, showing cell autonomous and non-autonomous effect of *fzr* loss *in vivo*. [**D(i)**] Control adult eye showing stereotypical pattern of compound eye. [**D(ii)**] Aberrant retina pattern observed in fzr^B mosaic adults. (**E**) MARCM mosaics generated as above stained with HRP (photoreceptor membrane). Magnified regions showing HRP boundary in dotted lines and glial cells stained with ani-Repo antibody. [**E(i)**] Control larval eye imaginal disc showing limitation of glial cells to the boundary set by HRP positive cells (boundary traced by white dotted lines).

(Continued)

lethality (Fig. 5A). Finally, we examined whether the patient *fzr* cDNA can rescue the CNS development defects in the $fzr^{T2A\text{-}GAL4}$ mutant embryos. The wild-type *fzr* cDNA was able to restore this defect (Fig. 5B–D), but the two variant cDNAs did not rescue the lesions (Fig. 5E and F). Together, the MARCM-based rescue experiments in the developing eye, overexpression analysis in the developing eye and rescue studies of embryonic neuronal developmental defects all suggest the variants found in three DEE patients act as strong hypomorphic alleles, impacting neuronal development in multiple contexts.

Discussion

In this study, we describe three individuals with DEE with childhood-onset generalized epilepsy carrying a *de novo* missense variant in *FZR1*. One missense variant affects the same amino acid residue as identified in a single previously published patient with DEE.[25] We further provide statistical and functional support for pathogenicity of these variants.

All four individuals carrying pathogenic *de novo FZR1* variants described so far suffer from neurodevelopmental delay and epilepsy, but with a broad phenotypic spectrum. While the previously reported individual had neonatal-onset treatment-resistant multifocal seizures, severe intellectual disability and prenatal microcephaly and was diagnosed with the DEE syndrome epilepsy of infancy with migrating focal seizures (EIMFS),[25] our study shows that the phenotypical spectrum also includes childhood-onset generalized seizure syndromes associated with moderate to severe intellectual disability, mild ataxia and normal head circumference. This variability could be due to strength of alleles or genetic backgrounds, which will require further investigation. Of note, two patients in our study were diagnosed with the epilepsy syndrome MAE. A normal development prior to seizure onset is historically considered a diagnostic criterion for the diagnosis of MAE, but the phenotypic boundaries of this syndrome remain debated.[55] In a recent study on the genetic aetiology of MAE, more than 20% of patients did have developmental delay prior to seizure onset.[8] This feature is indeed inherent to the concept of DEE, which acknowledges that the neurodevelopmental impairment of these patients is not solely related to frequent epileptic activity but is also a direct result of the underlying gene dysfunction. Of note, the 3-year-old Patient 3 in our study did not have (myoclonic) atonic seizures at time of inclusion in this study. As early disease history is very similar to Patient 2, carrying a variant leading to the same amino-acid substitution, further clinical evolution will tell whether other seizure types will still occur. Both patients also had similar signs of delayed myelination on early brain MRI. The more abundant epileptic activity and slow spike-wave activity in Patient 3 is, however, suggestive of a somewhat more severe disease course. In this respect, we cannot exclude the possibility that other rare genetic variants in brain-expressed genes contribute to the phenotype of Patient 3. Finally, all three patients in our study showed mild cerebellar ataxia, in the absence of cerebellar MRI abnormalities. Interestingly, and although FZR1 is ubiquitously expressed in the brain, the highest expression can be found in the cerebellum, where it has been shown to regulate cerebellar granule cell neurogenesis.[56]

All patients' variants are absent from the gnomAD database, and although we consider this supportive of pathogenicity, the authors realize that this evidence is hampered by the underrepresentation of populations sharing our patients' ethnicities (Turkish, Moroccan and Afghan) in this database. Absence from a database of Turkish exomes and genomes was determined, but the authors had no access to Moroccan or Afghan controls. However, absence of the variants in control populations is only one of the factors supporting the pathogenicity of the variants. There is a significant excess of both *de novo* and of (predicted) deleterious variants in our patient cohort of DEE patients compared to a control population such as gnomAD, suggesting an association of disease-causing *FZR1* variants and a DEE phenotype. Interestingly, all four DEE-associated variants described so far affect one of two different residues of FZR1. *FZR1* variants found in DEE patients affect residues that are likely to be important for the substrate recognition of Cdh1-APC.[10] Variants in this region may lead to altered substrate recognition and therefore lead to a diminished function of Cdh1-APC. Furthermore, we have shown that our patient variants lead to lower protein levels in human cell lines, which could indicate a reduction in the stability of mutant FZR1.

Using our *Drosophila* functional assays, we further show that both p.D187N and p.N333K variants lead to functional deficits in *fzr* (Cdh1) protein, especially in the developing nervous system. The DEE-associated variants fail to rescue photoreceptor pattern and glial cell migration that are phenotypes observed in previous *fzr* alleles in *Drosophila* and the patient variants behave as partial loss of function alleles. This is also observed in an overexpression assay in the developing eye, as we find that the variants display retention of some function compared to the reference allele. The difference in the functionality between the variants and the wild-type Fzr is dramatic in the embryonic CNS development as observed using the $fzr^{T2A\text{-}GAL4}$ allele, which might provide a more sensitive readout of functional differences. As a regulatory subunit of the E3 ubiquitin ligase complex APC, FZR1 (Cdh1) is involved in the turnover of many substrates.[57] One substrate of Cdh1-APC is FMRP (Fragile X mental Retardation Protein) encoded by the *FMR1* gene.[58] The interaction of FMRP with Cdh1-APC was shown to regulate metabotropic glutamate receptor (mGluR)-dependent synaptic plasticity[58] and the formation of stress granules and protein synthesis-dependent synaptic plasticity.[59] Triplet repeat expansion in *FMR1* causes Fragile X syndrome, a neurodevelopmental disorder often accompanied by seizures.[60] HECW2 (HECT, C2 And WW Domain Containing E3 Ubiquitin Protein Ligase 2, also known as NEDL2) is another substrate of Cdh1-APC[61] with a link to neurodevelopmental disorders, as *de novo* missense variants lead to intellectual disability, seizures and absent language.[61] Cdh1-APC-mediated degradation of HECW2 during mitotic exit is important for the regulation of metaphase to anaphase transition.[61] Abnormality of these or other substrates of Cdh1-APC may underlie the DEE and other phenotypes seen in our patients, which will require further molecular studies.

In summary, our work provides genetic, statistical and functional support for the role of *FZR1* in DEE, and we expand the phenotypic spectrum of *FZR1*-related encephalopathy from a severe syndrome with neonatal-onset EIMFS and microcephaly to include individuals with DEE with childhood-onset generalized

Figure 3 Continued
[E(ii)] fzr^{B} mosaics showing not only disturbances in HRP pattern but also migration of glial cells past the boundaries (arrowhead) of HRP-positive cells. **[E(iii)]** Eye imaginal discs showing rescue of HRP pattern and glial cell migration when *fzr* wild-type cDNA is overexpressed in mutant mosaics. **[E(iv)]** Eye imaginal discs showing glial migration in regions lacking HRP signal when *fzr* cDNA with variant p.D172N is overexpressed in *fzr* mutant cells. **[E(v)]** Eye imaginal discs showing similar defects in glial cell migration when *fzr* cDNA with variant p.N318K is expressed in *fzr* mutant cells.

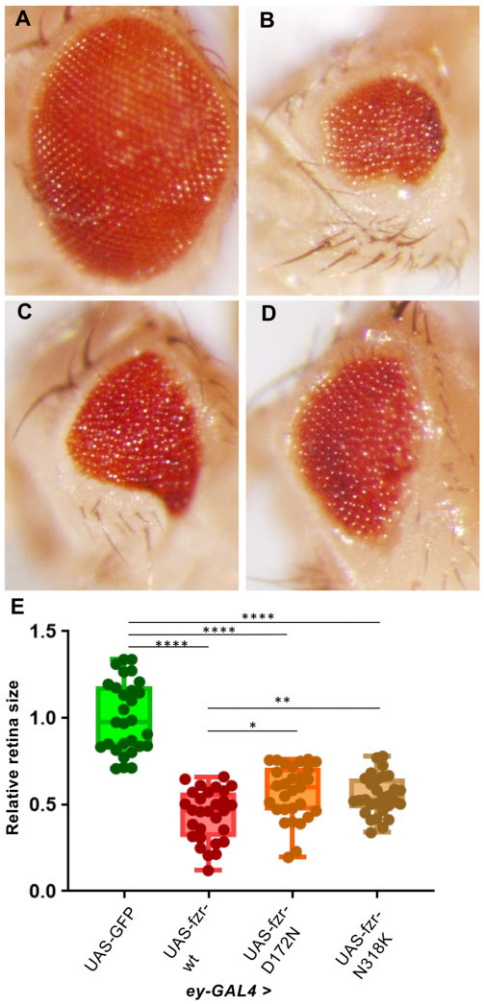

Figure 4 Overexpression of *fzr* leads to aberrant retinas. (**A**) Control ey3.5-GAL4 eyes showing stereotypical photoreceptor pattern and retina size. (**B**) Eyes of animals with wild-type fzr overexpressed using ey3.5-GAL4 showing severe eye size reduction and disrupted ommatidia pattern. (**C**) Adult eyes of ey3.5-GAL4 mediated overexpression of Fzr:p.D172N leading loss of photoreceptor pattern and reduction in retina size. (**D**) Adult eyes ey3.5-GAL4 mediated overexpression of Fzr:p.N318K leading to disruption in ommatidia pattern and reduction in eye size. (**E**) Box-and-whisker plot showing the quantitation of the eye size shows significant reduction of retina area due to the overexpression of wild-type or variant fzr cDNAs. Boxes are drawn from the 25th to the 75th percentiles, with a line indicating mean and error bars from maximum to minimum values. Reduction in the eye size due to variant overexpression is not as severe as defects caused by wild-type Fzr, which are statistically significant. Statistical difference evaluated using one-way ANOVA between all the samples followed by pair-wise analysis using Tukey's multiple comparison. Multiplicity corrected *P*-values indicated as $^{****}P < 0.0001$, $^{**}P < 0.001$, $^{*}P < 0.05$.

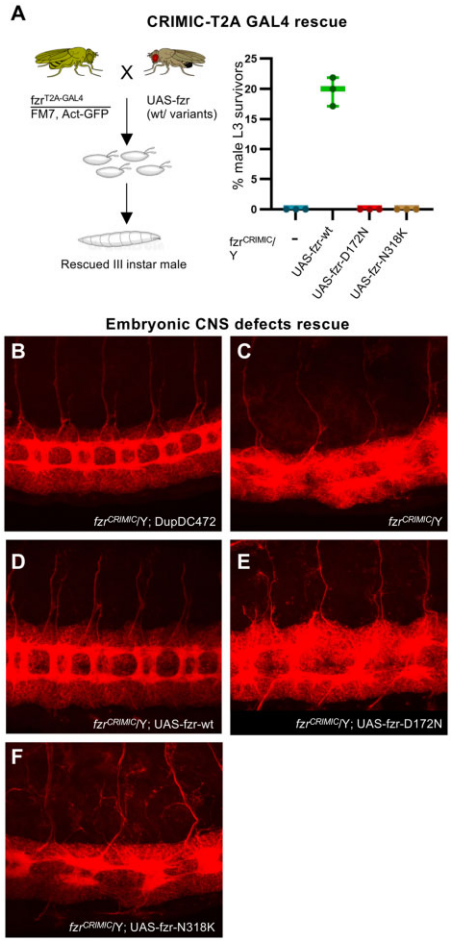

Figure 5 Embryonic CNS defects in fzrT2A-GAL4 mutants are not rescued by Fzr-carrying DEE patient variants. (**A**) Diagram showing the crossing scheme used to assess rescue of lethality observed in $fzr^{T2A\text{-}GAL4}$ using overexpression of wild-type or variant *Drosophila* Fzr and box-and-whisker plot showing the percentage of late third instar (L3) male larvae recovered by the overexpression of wild-type and variant cDNAs in a $fzr^{T2A\text{-}GAL4}$ mutant background. (**B**–**F**) *Drosophila* embryos at stage 15–16 showing neuronal membranes stained with HRP. (**B**) $fzr^{T2A\text{-}GAL4}$ hemizygous embryo ($fzr^{T2A\text{-}GAL4}$/Y) rescued with duplication of *fzr* genomic region on third chromosome serving as control. (**C**) $fzr^{T2A\text{-}GAL4}$/Y embryos showing severe defects in the pattern of neuron development. (**D**) Wild-type Fzr expression using the $fzr^{T2A\text{-}GAL4}$ rescues neuronal pattern. (**E** and **F**) $fzr^{T2A\text{-}GAL4}$ shows neurodevelopmental defects that are not rescued by the expression of Fzr p. \D172N or p.N318K.

epilepsies, mild ataxia and normal head circumference. The presence of early neurodevelopmental delay, even prior to seizure onset, is in line with the deleterious impact of patient variants on early neurodevelopment in a *Drosophila* model. The three molecularly defined *fzr* alleles (fzr^{A}, fzr^{B}, $fzr^{T2A\text{-}GAL4}$) are of great value to the study of the role of *fzr* in *Drosophila*, and due to the extensive conservation of residues, the study of *FZR1* in human diseases. The fly mutant, overexpression lines and assays that we have developed in this study will be an important asset for future studies on the role of *FZR1* in neurodevelopment and the impact of human disease variants on its interaction with substrates such as FMRP and HECW2 in the development of DEE.

Acknowledgements

We would like to thank Dr Michael Wangler for guidance on the bioinformatic analysis of the variants and comments and discussion on the manuscript.

Funding

N.S. is supported by the UA-Bijzonder Onderzoeksfonds (BOF)-DOCPRO4 (FFB180186). S.Y. is supported by the following grants from the National Institutes of Health (U54NS093793, R01DC014932, R24OD022005) and through funds provided by the

Nancy Chang PhD Award for Research Excellence, Baylor College of Medicine, and the Jan and Dan Duncan Neurological Research Institute at Texas Children's Hospital. S.W. is supported by the Fonds Wetenschappelijk onderzoek (FWO 1861419 N). H.M. is supported by the National Institutes of Health (R01 NS069605). H.J.B. is an investigator of the Howard Hughes Medical Institute (HHMI) and thanks HHMI for support.

Competing interests

The authors report no competing interests.

Supplementary material

Supplementary material is available at *Brain* online.

Appendix 1

Full details are provided in the Supplementary material.

Myoclonic Atonic Epilepsy (MAE) working group of the EuroEPINOMICS RES Consortium

Dana Craiu, Carol Davila, Ingo Helbig, Renzo Guerrini, Anna-Elina Lehesjoki, Carla Marini, Hiltrud Muhle, Rikke S Møller, Bernd Neubauer, Deb Pal, Katalin Sterbova, Pasquale Striano, Tiina Talvik, Sarah von Spiczak, Yvonne Weber, Dorota Hoffman-Zacharska.

References

1. Scheffer IE, Berkovic S, Capovilla G, et al. ILAE classification of the epilepsies: Position paper of the ILAE Commission for Classification and Terminology. *Epilepsia*. 2017;58(4):512–521.
2. Truty R, Patil N, Sankar R, et al. Possible precision medicine implications from genetic testing using combined detection of sequence and intragenic copy number variants in a large cohort with childhood epilepsy. *Epilepsia Open*. 2019;4(3):397–408.
3. McTague A, Howell KB, Cross JH, Kurian MA, Scheffer IE. The genetic landscape of the epileptic encephalopathies of infancy and childhood. *Lancet Neurol*. 2016;15(3):304–316.
4. Thomas RH, Berkovic SF. The hidden genetics of epilepsy—A clinically important new paradigm. *Nat Rev Neurol*. 2014;10(5):283–292.
5. Snoeijen-Schouwenaars FM, van Ool JS, Verhoeven JS, et al. Diagnostic exome sequencing in 100 consecutive patients with both epilepsy and intellectual disability. *Epilepsia*. 2019;60(1):155–164.
6. Demos M, Guella I, DeGuzman C, et al. Diagnostic yield and treatment impact of targeted exome sequencing in early-onset epilepsy. *Front Neurol*. 2019;10:434.
7. Larsen J, Johannesen KM, Ek J, et al. The role of SLC2A1 mutations in myoclonic astatic epilepsy and absence epilepsy, and the estimated frequency of GLUT1 deficiency syndrome. *Epilepsia*. 2015;56(12):e203-8.
8. Tang S, Addis L, Smith A, et al. Phenotypic and genetic spectrum of epilepsy with myoclonic atonic seizures. *Epilepsia*. 2020;61(5):995–1007.
9. Sobreira N, Schiettecatte F, Valle D, Hamosh A. GeneMatcher: A matching tool for connecting investigators with an interest in the same gene. *Human Mutation*. 2015;36(10):928–930.
10. Chang LF, Zhang Z, Yang J, McLaughlin SH, Barford D. Molecular architecture and mechanism of the anaphase-promoting complex. *Nature*. 2014;513(7518):388–393.
11. Fang G, Yu H, Kirschner MW. Direct binding of CDC20 protein family members activates the anaphase-promoting complex in mitosis and G1. *Mol Cell*. 1998;2(2):163–171.
12. Sudo T, Ota Y, Kotani S, et al. Activation of Cdh1-dependent APC is required for G1 cell cycle arrest and DNA damage-induced G2 checkpoint in vertebrate cells. *EMBO J*. 2001;20(22):6499–6508.
13. García-Higuera I, Manchado E, Dubus P, et al. Genomic stability and tumour suppression by the APC/C cofactor Cdh1. *Nat Cell Biol*. 2008;10(7):802–811.
14. Delgado-Esteban M, Garcia-Higuera I, Maestre C, Moreno S, Almeida A. APC/C-Cdh1 coordinates neurogenesis and cortical size during development. *Nat Commun*. 2013;4:2879.
15. Huang J, Bonni A. A decade of the anaphase-promoting complex in the nervous system. *Genes Dev*. 2016;30(6):622–638.
16. Li J, Chen X, Li X, et al. Upregulation of Cdh1 in the trigeminal spinal subnucleus caudalis attenuates trigeminal neuropathic pain via inhibiting GABAergic neuronal apoptosis. *Neurochem Int*. 2020;133:104613.
17. Li Z, Zhang B, Yao W, Zhang C, Wan L, Zhang Y. APC-Cdh1 regulates neuronal apoptosis through modulating glycolysis and pentose-phosphate pathway after oxygen-glucose deprivation and reperfusion. *Cell Mol Neurobiol*. 2019;39(1):123–135.
18. Neuert H, Yuva-Aydemir Y, Silies M, Klambt C. Different modes of APC/C activation control growth and neuron–glia interaction in the developing *Drosophila* eye. *Development*. 2017;144(24):4673–4683.
19. Bobo-Jimenez V, Delgado-Esteban M, Angibaud J, et al. APC/C(Cdh1)-Rock2 pathway controls dendritic integrity and memory. *Proc Natl Acad Sci USA*. 2017;114(17):4513–4518.
20. Silies M, Klambt C. APC/C(Fzr/Cdh1)-dependent regulation of cell adhesion controls glial migration in the *Drosophila* PNS. *Nat Neurosci*. 2010;13(11):1357–1364.
21. Sigrist SJ, Lehner CF. *Drosophila* fizzy-related down-regulates mitotic cyclins and is required for cell proliferation arrest and entry into endocycles. *Cell*. 1997;90(4):671–681.
22. Pimentel AC, Venkatesh TR. *rap* gene encodes Fizzy-related protein (Fzr) and regulates cell proliferation and pattern formation in the developing *Drosophila* eye-antennal disc. *Dev Biol*. 2005;285(2):436–446.
23. Yamamoto S, Jaiswal M, Charng WL, et al. A drosophila genetic resource of mutants to study mechanisms underlying human genetic diseases. *Cell*. 2014;159(1):200–214.
24. Karpilow J, Kolodkin A, Bork T, Venkatesh T. Neuronal development in the *Drosophila* compound eye: Rap gene function is required in photoreceptor cell R8 for ommatidial pattern formation. *Genes Dev*. 1989;3(12A):1834–1844.
25. Rodriguez C, Sanchez-Moran I, Alvarez S, et al. A novel human Cdh1 mutation impairs anaphase promoting complex/cyclosome activity resulting in microcephaly, psychomotor retardation, and epilepsy. *J Neurochem*. 2019;151(1):103–115.
26. Lee PT, Zirin J, Kanca O, et al. A gene-specific T2A-GAL4 library for drosophila. *Elife*. 2018;7:e35574.
27. Suls A, Jaehn JA, Kecskes A, et al. *De novo* loss-of-function mutations in CHD2 cause a fever-sensitive myoclonic epileptic encephalopathy sharing features with Dravet syndrome. *Am J Hum Genet*. 2013;93(5):967–975.
28. Lek M, Karczewski KJ, Minikel EV, et al. Analysis of protein-coding genetic variation in 60,706 humans. *Nature*. 2016;536(7616):285–291.
29. Karczewski KJ, Francioli LC, Tiao G, et al. The mutational constraint spectrum quantified from variation in 141,456 humans. *Nature*. 2020;581(7809):434–443.

30. Human Genomics. The Genotype–Tissue Expression (GTEx) pilot analysis: Multitissue gene regulation in humans. *Science (New York, NY)*. 2015;348(6235):648–660.
31. Rentzsch P, Witten D, Cooper GM, Shendure J, Kircher M. CADD: Predicting the deleteriousness of variants throughout the human genome. *Nucleic Acids Res*. 2019;47(D1):D886–D894.
32. Carvill GL, McMahon JM, Schneider A, et al. Mutations in the GABA transporter SLC6A1 cause epilepsy with myoclonic–atonic seizures. *Am J Hum Genet*. 2015;96(5):808–815.
33. Kumar P, Henikoff S, Ng PC. Predicting the effects of coding non-synonymous variants on protein function using the SIFT algorithm. *Nat Protocols*. 2009;4(7):1073–1081.
34. Adzhubei IA, Schmidt S, Peshkin L, et al. A method and server for predicting damaging missense mutations. *Nat Methods*. 2010;7(4):248–249.
35. Haelterman NA, Jiang L, Li Y, et al. Large-scale identification of chemically induced mutations in *Drosophila melanogaster*. *Genome Res*. 2014;24(10):1707–1718.
36. Nagarkar-Jaiswal S, Manivannan SN, Zuo Z, Bellen HJ. A cell cycle-independent, conditional gene inactivation strategy for differentially tagging wild-type and mutant cells. *Elife*. 2017;6:e26420.
37. Ware JS, Samocha KE, Homsy J, Daly MJ. Interpreting *de novo* variation in human disease using denovolyzeR. *Curr Protoc Hum Genet*. 2015;87:7.25.1–7.25.15.
38. McLaren W, Gil L, Hunt SE, et al. The ensembl variant effect predictor. *Genome Biol*. 2016;17(1):122.
39. Schindelin J, Arganda-Carreras I, Frise E, et al. Fiji: An open-source platform for biological-image analysis. *Nat Methods*. 2012;9(7):676–682.
40. Lee HS, Kim MW, Jin KS, et al. Molecular analysis of the interaction between human PTPN21 and the oncoprotein E7 from human papillomavirus genotype 18. *Mol Cells*. 2021;44(1):26–37.
41. Campbell JS, Davidson AJ, Todd H, et al. PTPN21/Pez is a novel and evolutionarily conserved key regulator of inflammation *in vivo*. *Curr Biol*. 2021;31(4):875–883.e5.
42. Chen J, Lee G, Fanous AH, et al. Two non-synonymous markers in PTPN21, identified by genome-wide association study data-mining and replication, are associated with schizophrenia. *Schizophrenia Res*. 2011;131(1-3):43–51.
43. Siddiqui N, Zwetsloot AJ, Bachmann A, et al. PTPN21 and Hook3 relieve KIF1C autoinhibition and activate intracellular transport. *Nat Commun*. 2019;10(1):2693.
44. Plani-Lam JH, Chow TC, Siu KL, et al. PTPN21 exerts pro-neuronal survival and neuritic elongation via ErbB4/NRG3 signaling. *Int J Biochem Cell Biol*. 2015;61:53–62.
45. Larocque G, La-Borde PJ, Clarke NI, Carter NJ, Royle SJ. Tumor protein D54 defines a new class of intracellular transport vesicles. *J Cell Biol*. 2020;219(1):e201812044.
46. Mukudai Y, Kondo S, Fujita A, Yoshihama Y, Shirota T, Shintani S. Tumor protein D54 is a negative regulator of extracellular matrix-dependent migration and attachment in oral squamous cell carcinoma-derived cell lines. *Cell Oncol (Dordrecht)*. 2013;36(3):233–245.
47. Stirnimann CU, Petsalaki E, Russell RB, Muller CW. WD40 proteins propel cellular networks. *Trends Biochem Sci*. 2010;35(10):565–574.
48. Kanca O, Andrews JC, Lee PT, et al. *De novo* variants in WDR37 are associated with epilepsy, colobomas, dysmorphism, developmental delay, intellectual disability, and cerebellar hypoplasia. *Am J Hum Genet*. 2019;105(2):413–424.
49. Newsome TP, Asling B, Dickson BJ. Analysis of *Drosophila* photoreceptor axon guidance in eye-specific mosaics. *Development*. 2000;127(4):851–860.
50. Lee T, Luo L. Mosaic analysis with a repressible cell marker (MARCM) for *Drosophila* neural development. *Trends Neurosci*. 2001;24(5):251–254.
51. Yao KM, Samson ML, Reeves R, White K. Gene *elav* of *Drosophila melanogaster*: A prototype for neuronal-specific RNA binding protein gene family that is conserved in flies and humans. *J Neurobiol*. 1993;24(6):723–739.
52. Lee T, Luo L. Mosaic analysis with a repressible cell marker for studies of gene function in neuronal morphogenesis. *Neuron*. 1999;22(3):451–461.
53. Heuser K, Szokol K, Taubøll E. The role of glial cells in epilepsy. *Tidsskr Nor Laegeforening*. 2014;134(1):37–41.
54. Nickels K. Epilepsy with myoclonic atonic seizures: Why is the yield of genetic testing for a 'presumed genetic' epilepsy low? *Epilepsy Curr*. 2020;20(6):351–352.
55. Penas C, Govek EE, Fang Y, et al. Casein kinase 1δ is an APC/C(Cdh1) substrate that regulates cerebellar granule cell neurogenesis. *Cell Rep*. 2015;11(2):249–260.
56. Zhou Z, He M, Shah AA, Wan Y. Insights into APC/C: From cellular function to diseases and therapeutics. *Cell Div*. 2016;11:9.
57. Huang J, Ikeuchi Y, Malumbres M, Bonni A. A Cdh1-APC/FMRP ubiquitin signaling link drives mGluR-dependent synaptic plasticity in the mammalian brain. *Neuron*. 2015;86(3):726–739.
58. Valdez-Sinon AN, Lai A, Shi L, et al. Cdh1-APC regulates protein synthesis and stress granules in neurons through an FMRP-dependent mechanism. *iScience*. 2020;23(5):101132.
59. Verkerk AJ, Pieretti M, Sutcliffe JS, et al. Identification of a gene (FMR-1) containing a CGG repeat coincident with a breakpoint cluster region exhibiting length variation in fragile X syndrome. *Cell*. 1991;65(5):905–914.
60. Lu L, Hu S, Wei R, et al. The HECT type ubiquitin ligase NEDL2 is degraded by anaphase-promoting complex/cyclosome (APC/C)-Cdh1, and its tight regulation maintains the metaphase to anaphase transition. *J Biol Chem*. 2013;288(50):35637–35650.
61. Berko ER, Cho MT, Eng C, et al. *De novo* missense variants in HECW2 are associated with neurodevelopmental delay and hypotonia. *J Med Genet*. 2017;54(2):84–86.